Neuron, Vol. 22, 243–252, February, 1999, Copyright ©1999 by Cell Press

Retarded Growth and Deficits in the Enteric and Parasympathetic Nervous System in Mice Lacking GFRα2, a Functional Neurturin Receptor

Jari Rossi,* Keijo Luukko,† Dmitry Poteryaev,* Antti Laurikainen,*§ Yun Fu Sun,* Tiina Laakso,* Simo Eerikäinen,* Raimo Tuominen,§ Merja Lakso,‡ Heikki Rauvala,*‡‖ Urmas Arumäe,* Michael Pasternack,*§ Mart Saarma,* and Matti S. Airaksinen*#

*Program of Molecular Neurobiology
†Program of Developmental Biology
‡Transgene Unit
Institute of Biotechnology
§Department of Pharmacy
Division of Pharmacology and Toxicology
‖Department of Biosciences
Viikki Biocenter
FIN-00014 University of Helsinki
Finland

Summary

Glial cell line–derived neurotrophic factor (GDNF) and a related protein, neurturin (NTN), require a GPI-linked coreceptor, either GFRα1 or GFRα2, for signaling via the transmembrane Ret tyrosine kinase. We show that mice lacking functional GFRα2 coreceptor (*Gfra2*$^{-/-}$) are viable and fertile but have dry eyes and grow poorly after weaning, presumably due to malnutrition. While the sympathetic innervation appeared normal, the parasympathetic cholinergic innervation was almost absent in the lacrimal and salivary glands and severely reduced in the small bowel. Neurite outgrowth and trophic effects of NTN at low concentrations were lacking in *Gfra2*$^{-/-}$ trigeminal neurons in vitro, whereas responses to GDNF were similar between the genotypes. Thus, GFRα2 is a physiological NTN receptor, essential for the development of specific postganglionic parasympathetic neurons.

Introduction

Glial cell line–derived neurotrophic factor (GDNF) and a related factor, neurturin (NTN), show similar survival-promoting activities on many central and peripheral neurons, including sensory, sympathetic, motor, and midbrain dopamine neurons (Lin et al., 1993; Henderson et al., 1994; Buj-Bello et al., 1995; Trupp et al., 1995; Kotzbauer et al., 1996; Horger et al., 1998). Both GDNF and NTN signal via a multicomponent receptor complex, which consists of the Ret tyrosine kinase (Durbec et al., 1996b; Trupp et al., 1996) and a glycosyl-phosphotidylinositol- (GPI-) linked, ligand-binding α component, either GDNF family receptor α1 (GFRα1) or GFRα2 (Jing et al., 1996, 1997; Treanor et al., 1996; Baloh et al., 1997; Buj-Bello et al., 1997; Klein et al., 1997; Sanicola et al., 1997; Suvanto et al., 1997). Results from in vitro assays suggest that GDNF preferentially uses GFRα1 and NTN uses GFRα2 as the coreceptor. However, there is a degree of promiscuity in the ligand specificities of GFRα's, and there are differences in how they activate Ret (Baloh et al., 1997; Buj-Bello et al., 1997; Creedon et al., 1997; Jing et al., 1997; Klein et al., 1997; Sanicola et al., 1997; Suvanto et al., 1997; Trupp et al., 1998).

Recently, additional Ret-signaling components in the GDNF family have been identified: artemin (Baloh et al., 1998b), which signals through GFRα3, a more distantly related α receptor (Baloh et al., 1998a; Jing et al., 1998; Masure et al., 1998; Naveilhan et al., 1998; Nomoto et al., 1998; Trupp et al., 1998; Worby et al., 1998); and persephin (Milbrandt et al., 1998), which seems to be a ligand for GFRα4 (Enokido et al., 1998), an α component related to GFRα1 and GFRα2 (Thompson et al., 1998). Neither artemin nor persephin seems to signal through GFRα2 (Baloh et al., 1998b; Milbrandt et al., 1998).

Transcripts of different *Gfra*s are present in temporally and spatially distinct, but partially overlapping, subpopulations of cells (e.g., Naveilhan et al., 1998). *Gfra*s are usually coexpressed with *Ret* that is complementary to the expression of their ligand mRNAs in different types of cells (Luukko et al., 1997; Widenfalk et al., 1997; Golden et al., 1998; Naveilhan et al., 1998; Trupp et al., 1998; Yu et al., 1998). Mice lacking GDNF, GFRα1, or Ret all die soon after birth and share a similar phenotype of kidney agenesis and absence of enteric neurons below the stomach, although some differences are found, for example, in sympathetic ganglia (Schuchardt et al., 1994; Moore et al., 1996; Pichel et al., 1996; Sánchez et al., 1996; Cacalano et al., 1998; Enomoto et al., 1998). Analogous to *Gdnf* and *Gfra1* in kidney, *Ntn* and *Gfra2* show spatially complementary expression in some non-neuronal tissues, such as developing teeth and salivary gland (Luukko et al., 1997; Widenfalk et al., 1997). In some regions, the *Gfra*s are expressed without *Ret* (e.g., *Gfra2* in adult brain), suggesting that the α receptors may have roles of their own or interact with Ret in *trans* (Trupp et al., 1997; Yu et al., 1998).

To assess the in vivo function of GFRα2 and the physiological relevance of its ligand specificity, we have produced mice lacking functional GFRα2 receptor (*Gfra2*$^{-/-}$). The mice exhibit profound deficits in the cholinergic innervation of the lacrimal and salivary glands, as well as the small intestine, but not in some other parasympathetic target areas. The mice have dry eyes and grow poorly after weaning, presumably due to alimentary tract dysfunction and malnutrition. Neuritogenesis and survival of embryonic trigeminal neurons at low NTN concentrations were prominent in wild-type but almost absent in *Gfra2*$^{-/-}$ mice, whereas responses to GDNF were similar. Thus, GFRα2 mediates biological responses of NTN and is essential for the development of distinct enteric and parasympathetic neurons.

Results and Discussion

Generation of the *Gfra2*$^{-/-}$ Mice

A predicted *Gfra2* null allele was created by deleting part of the first coding exon (exon 1; Baloh et al., 1998a),

#To whom correspondence should be addressed (e-mail: matti.airaksinen@helsinki.fi).

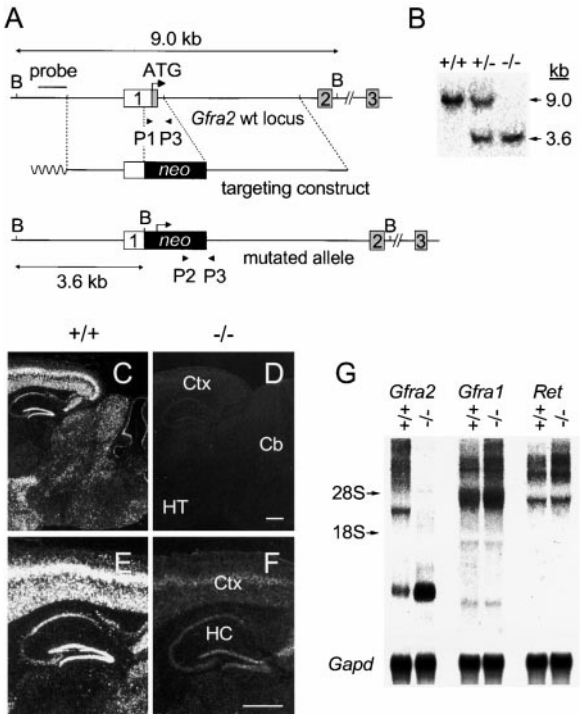

Figure 1. Targeted Inactivation of *Gfra2*

(A) Structure of mouse *Gfra2* locus, replacement targeting vector, and mutant alleles. Relative positions of exons 1–3 (Baloh et al., 1998a) are indicated, coding parts in gray. Closed arrowheads denote primer pairs used for genotyping with PCR. B, BamH1.

(B) Southern analysis of mice tails with a 5′ outside probe indicated in (A) illustrating the 9 kb wild-type and 3.6 kb targeted allele hybridizing bands following BamH1 digestion.

(C–F) In situ hybridization of brain sections of adult wild-type (C and E) and *Gfra2*$^{-/-}$ (D and F) mice with exon 1 (C and D) and full-length (E and F) *Gfra2* probes. Cb, cerebellum; Ctx, cortex; HC, hippocampus; HT, hypothalamus. Scale bars, 200 μm.

(G) Northern blot analysis of total brain RNA from wild-type (+/+) and *Gfra2*$^{-/-}$ (−/−) mice. Hybridization with a mouse *Gfra2* probe spanning exons 2 and 3 reveals several transcripts of various sizes in wild-type mice, whereas *Gfra2*$^{-/-}$ mice lack all the mRNAs, except an upregulated transcript of about 0.5 kb. Analysis of *Gfra1* and *Ret* mRNA expression showed no apparent difference between the genotypes. The amounts of total RNA in samples were normalized by probing for *Gapd*.

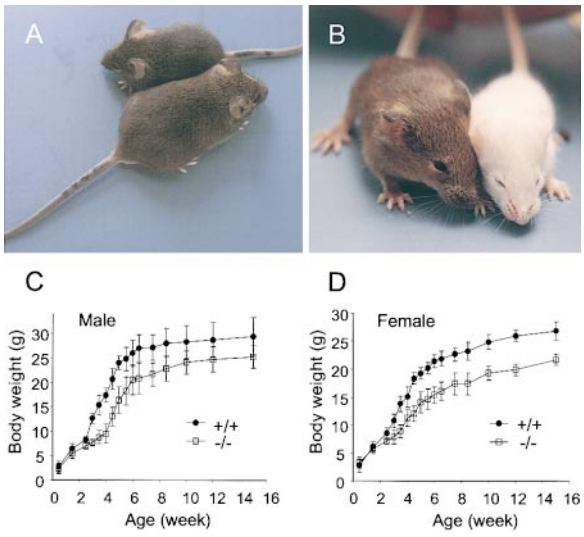

Figure 2. Poor Growth and Apparent Ptosis in *Gfra2*$^{-/-}$ Mice

(A and B) Photographs of 4-week-old male wild-type mice ([A], lower; [B], left) and their smaller *Gfra2*$^{-/-}$ littermates. Note apparent ptosis-like phenotype (dropping eyelids) in the mutant animal ([B], right).

(C and D) Growth curves of male and female mice. The value of each point is the average body weight (± SD) of three to five mice from wild-type and their *Gfra2*$^{-/-}$ littermate pairs that were followed for 16 weeks. The difference in weight becomes apparent at the age of 2–3 weeks and is most prominent in the 4-week-old males. A significant difference remains beyond 4 months of age in both sexes.

which includes the translation initiation site and signal sequence of the *Gfra2* gene, using homologous recombination in embryonic stem cells (Figures 1A and 1B). Chimeric mice, derived from these cells, were bred to C57BL/6 and 129/Sv females to establish heterozygotes (*Gfra2*$^{+/-}$). Of 250 offspring from *Gfra2*$^{+/-}$ intercrosses typed after weaning, 57 (23%) were *Gfra2*$^{-/-}$, 125 (50%) were *Gfra2*$^{+/-}$, and 68 (27%) were wild type, indicating no increased lethality in the homozygous animals.

In situ hybridization analysis of adult mouse brain and E18 embryos with *Gfra2* exon 1 probe revealed strong expression in wild-type animals but no labeling in the *Gfra2*$^{-/-}$ mice (Figures 1C and 1D; data not shown). An identical expression pattern was seen in wild-type mice using a full-length *Gfra2* probe, which also revealed a similar but much weaker expression in the mutant animals (Figures 1E and 1F), suggesting the presence of a transcript under the control of the *Gfra2* promoter. Northern blot analysis of brain using a *Gfra2* probe spanning exons 2 and 3 (Figure 1G) and a full-length probe (data not shown) indicated that the large wild-type transcripts were absent in *Gfra2*$^{-/-}$ mice but a short mRNA species of about 0.5 kb was upregulated, consistent with the in situ hybridization result. RT–PCR analysis of various tissues confirmed that this transcript does not include exon 1 but includes exons 2 and 3 (data not shown). In the absence of a signal sequence, a hypothetical translation of this transcript would lead to a short, nonglycosylated, cytoplasmic peptide unable to bind any extracellular ligands or receptors. Sequencing of several clones of the *Gfra2* transcript from *Gfra2*$^{-/-}$ mice indicated a rearrangement of exons, producing a frameshift with early stop codons. Taken together, the *Gfra2*$^{-/-}$ mice most likely represent a true null allele.

Expression of *Gdnf*, *Ntn*, *Gfra1*, and *Ret* in E18 embryos and adult brains was similar between the genotypes as analyzed by Northern blot and in situ hybridization (Figure 1G; data not shown), suggesting that the expression of other Ret-signaling components is not regulated via GFRα2. This also implies that in the absence of GFRα2, the *Ret*-expressing cells largely survive and that there are no obvious compensatory changes in *Gdnf* or *Gfra1* expression to account for this cell survival.

The *Gfra2*$^{-/-}$ Mice Exhibit an Apparent Ptosis and Become Retarded in Growth Postnatally

Gfra2$^{-/-}$ mice appeared normal in size at birth, but at weaning they were consistently smaller than their wild-type littermates (Figure 2A), and many of them kept

their eyes partially closed, displaying an apparent ptosis (Figure 2B). Growth failure of *Gfra2*$^{-/-}$ mice became evident at the age of 2–3 weeks and was most pronounced at 4–6 weeks, when the difference in weight between the genotypes was 30%–50% (Figures 2C and 2D). At this age, the knockout animals could be easily distinguished from wild-type animals based on size alone. During the following months, the mutants showed some catch-up growth but still remained about 20% smaller than their wild-type littermates at 4 months of age. Changes in nose–tail length, with a maximal difference of 10%–15%, were less severe than changes in weight. Similar growth retardation was seen in three mutant lines and in both 129/Sv and C57BL/6 backgrounds but not in *Gfra2*$^{+/-}$ animals. In the hybrid background, *Gfra2*$^{-/-}$ mice have been viable and fertile up to 12 months of age. Litters from homozygote intercrosses have a normal number of pups, which also develop similar postnatal growth retardation and eye phenotypes.

Consistent with the growth retardation, most organs were smaller and weighed 30%–50% less in the mutants at 4–6 weeks. The brain size was relatively well maintained, being reduced only by 5%–20% in weight. Except for delayed development, routine histological analysis of the mutants did not reveal obvious defects in major organs, including kidney, spleen, liver, and lung (data not shown). *Gfra2* is abundantly expressed in many regions of the adult brain, including the olfactory bulb, cortex, and hypothalamus (Figure 1C; Golden et al., 1998). However, the normal expression pattern of the small transcript (Figure 1F) suggests that most of these neurons are preserved in the *Gfra2*$^{-/-}$ brain. Moreover, an immunohistological survey with several neuronal markers (choline acetyltransferase, calbindin, calretinin, parvalbumin, neuropeptide Y, olfactory marker protein, tyrosine hydroxylase, and neurofilament chains) failed to demonstrate any gross defects in the central nervous system of the mutants (data not shown).

Gfra2$^{-/-}$ Mice Have Dry Eyes and Lack Cholinergic Innervation of the Lacrimal and Salivary Glands

The apparent ptosis in *Gfra2*$^{-/-}$ mice was variable: in many animals it was unilateral with increased blinking of the other eye, and many mice blinked or kept their lids down only part of the time. The upper eyelid is elevated by the levator palpebrae superioris muscle (LPSM) innervated by the oculomotor nerve and by the superior tarsal muscle (STM) innervated by sympathetic nerves. *Gfra2* and *Ret* are expressed in sympathetic (Durbec et al., 1996a; Widenfalk et al., 1997) and oculomotor neurons (Golden et al., 1998), suggesting a possible role for GFRα2 signaling in the innervation of eyelid muscles. However, no difference in the density of tyrosine hydroxylase-positive fibers in the STM (Figures 3A and 3B) was observed between the genotypes ($n = 3$), and analysis of the oculomotor nerves demonstrated a similar number (*Gfra2*$^{-/-}$ 680 $\pm$ 40, versus wild-type 730 $\pm$ 60, $n = 4$ for both genotypes, $p > 0.05$) and size distribution (data not shown) of myelinated fibers. In addition, the number and morphology of oculomotor nerve endplates on LPSM were similar (data not shown).

An increased blink rate could be caused by dry eyes,

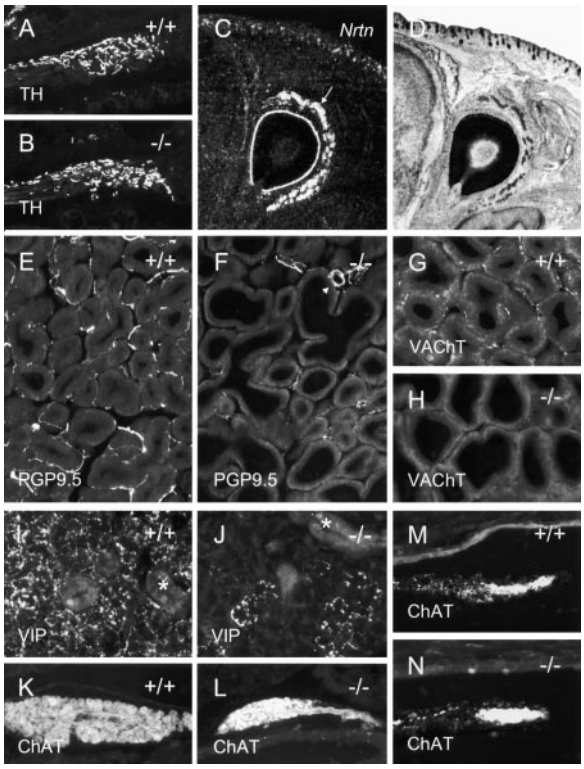

Figure 3. *Gfra2*$^{-/-}$ Mice Lack Cholinergic Innervation of the Lacrimal and Salivary Glands

(A and B) The sympathetic (TH-immunopositive) innervation of the upper eyelid muscle is similar in wild-type ([A], +/+) and *Gfra2*$^{-/-}$ ([B], −/−) mice.

(C and D) Expression of *Ntn* in the developing lacrimal glands (arrow). In situ hybridization of a sagittal section through E18 mouse head with *Ntn* probe shown in dark (C) and bright field (D).

(E and F) PGP9.5-immunoreactive nerve fibers surround each acinus in wild-type (E) lacrimal glands, whereas most acini from *Gfra2*$^{-/-}$ mice (F) lack innervation. The innervation of blood vessels (arrowhead) is intact. Note the atrophy of acinus cells and dilatation of acini.

(G and H) Parasympathetic cholinergic innervation of the wild-type (G) and *Gfra2*$^{-/-}$ (H) lacrimal glands stained for vesicular acetylcholine transporter (VAChT).

(I and J) Parasympathetic (VIP-positive) nerve fibers in the sublingual salivary gland. A dense network of fibers surrounds all the acini in wild-type mice (I), whereas only a minority of mutant acini (J) are innervated. Asterisks denote connecting secretory tubules.

(K and L) Representative sections through the submandibular ganglion stained for ChAT. The size of the ganglion from *Gfra2*$^{-/-}$ mutant mice (L) is clearly smaller than its wild-type counterpart (K).

(M and N) Parasympathetic innervation of the pupillary constrictor muscle is similar between the genotypes (ChAT immunostaining).

which could also explain why many animals preferred to keep their eyes closed. *Ntn* was highly expressed in developing lacrimal gland (Figures 3C and 3D), and *Gfra2* and *Ret* transcripts are present in developing parasympathetic ganglia (Nosrat et al., 1997; data not shown). Immunostaining with PGP9.5, a panneuronal marker, showed an almost complete lack of lacrimal gland innervation in *Gfra2*$^{-/-}$ mice (Figures 3E and 3F). Whereas the sympathetic innervation around the blood vessels was intact, the cholinergic parasympathetic fibers were virtually absent (Figures 3G and 3H). Moreover, the acinar cells appeared atrophied and the acini

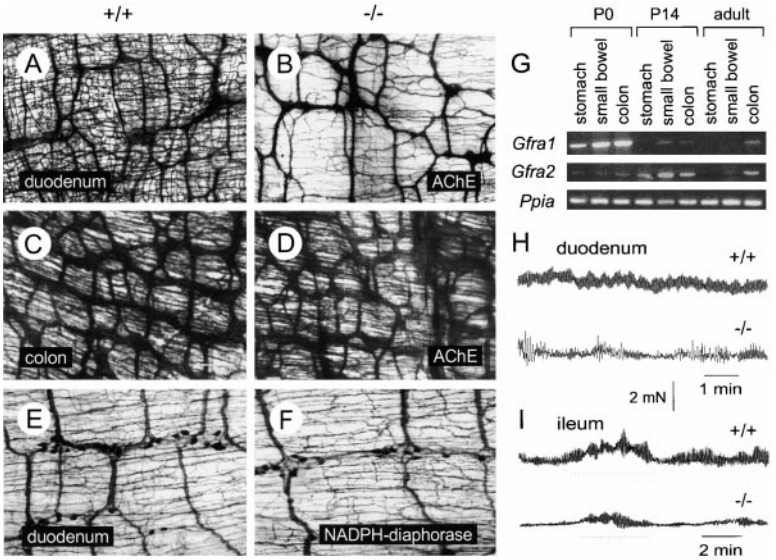

Figure 4. Analysis of the Gut: Innervation of Myenteric Plexus, Expression of α Receptors, and Motility In Vitro

(A–D) Acetylcholinesterase staining of duodenum (A and B) and colon (C and D) from 6-week-old littermates. In wild-type (+/+) gut, the myenteric plexus forms a fine fiber network, which is clearly reduced in the duodenum and ileum but not in colon of *Gfra2*$^{-/-}$ (−/−) mice.

(E and F) NADPH-diaphorase staining of duodenum. No difference in the density of fibers of cell bodies is observed between wild-type (+/+) and *Gfra2*$^{-/-}$ (−/−) mice.

(G) Ethidium bromide–stained gels showing RT–PCR products for *Gfra1* and *Gfra2* from stomach, small bowel, and colon of postnatal day P0, P14, and adult wild-type mice. *Gfra1* expression is downregulated in postnatal gut, whereas *Gfra2* levels are upregulated in P14 bowel. Bottom line shows that the tissues contain similar levels of control *Ppia* transcript. Similar results were obtained from a separate set of tissues.

(H and I) Spontaneous contractile activity of wild-type (+/+) and *Gfra2*$^{-/-}$ (−/−) duodenum (H) and ileum (I). There is a marked difference in contractile activity between the genotypes, the wild type displaying more robust contractions and a more pronounced "waxing and waning" pattern. The dotted line is drawn to mark the regularly occurring TTX-sensitive contraction increase, which was always less pronounced in the mutants.

enlarged (Figures 3E–3H). Preliminary analysis indicated that tear secretion (see Experimental Procedures) was significantly reduced in the mutant mice ($p < 0.01$, $n = 4$). Thus, lack of GFRα2 leads to a dry eye syndrome due to lack of lacrimal gland innervation.

We also observed a dramatic reduction of cholinergic parasympathetic innervation in the sublingual (Figures 3I and 3J) and parotid salivary glands (data not shown), which express *Ntn* and *Gfra2* during development (Widenfalk et al., 1997; data not shown). Concordant with the reduced target innervation in adult *Gfra2*$^{-/-}$ mice, the number of submandibular ganglion neurons (Figures 3K and 3L) was reduced by 81% ± 6% ($n = 4$, $p < 0.001$). Interestingly, developing submandibular neurons in vitro are sensitive to NTN and do not require GFRα1 (Cacalano et al., 1998). In contrast, cholinergic innervation of the pupillary constrictor muscle (Figures 3M and 3N) from the ciliary ganglion and the pupillary reflex (data not shown) were intact in *Gfra2*$^{-/-}$ mice. Taken together, the results indicate that many, but not all, preganglionic parasympathetic neurons in the head region critically require GFRα2-mediated signaling. Future studies should compare the development and target innervation of different parasympathetic ganglia of *Gfra2*$^{-/-}$ and *Ret*$^{-/-}$ mice in more detail.

Deficient Cholinergic Myenteric Plexus of the Small Intestine in *Gfra2*$^{-/-}$ Mice

In mouse intestine, the temporal expression of GDNF, NTN, and their receptor components is complementary. While the expression of *Gdnf* and *Gfra1* is abundant early in embryonic gut (Moore et al., 1996; Cacalano et al., 1998), they appear undetectable in adult duodenum (Naveilhan et al., 1998). *Gdnf* mRNA is found in the muscle layers of the developing gut wall (Moore et al., 1996; Suvanto et al., 1996), whereas *Ret* (Pachnis et al., 1993) and *Gfra1* (Cacalano et al., 1998) are expressed in the ganglia of both myenteric and submucous plexuses. In contrast, the expression of *Gfra2* and *Ntn* is low in early embryonic gut but increases later (Baloh et al., 1997; Widenfalk et al., 1997; Naveilhan et al., 1998). Interestingly, *Ntn* is expressed exclusively in the circular muscle layer, whereas *Gfra2* mRNA is expressed in the ganglia of myenteric but not submucosal plexus (Widenfalk et al., 1997).

The distinct expression pattern of *Gfra2* in the gut and a report that mice lacking NTN have reduced density of acetylcholinesterase- (AChE-) positive fibers in the myenteric plexus of duodenum (J. Milbrandt, personal communication), prompted us to analyze the gut innervation of *Gfra2*$^{-/-}$ mice in whole mounts. In the myenteric plexus of adult *Gfra2*$^{-/-}$ mice, the density of fine AChE-positive fiber network, but not the thick nerve tracts, was always ($n = 8$ littermate pairs, ages 1–3 months) clearly reduced in the duodenum (Figures 4A and 4B) and ileum (data not shown) but not so clearly in the colon (Figures 4C and 4D) or stomach (data not shown). Quantification indicated a 45%, 35%, and 15% decrease in fiber density in duodenum, jejunum, and colon, respectively, of *Gfra2*$^{-/-}$ mice ($n = 3$–5 for each tissue, $p < 0.005$ for duodenum). Myenteric preparations were also stained with whole-mount NADPH-diaphorase histochemistry (Figures 4E and 4F) that labels the nitric oxide synthase–containing (nitrergic) neurons. The density of nitrergic fibers (33 ± 6 versus 35 ± 3) and neuronal cell bodies (73 ± 10 versus 65 ± 8) in the duodenum was similar between wild-type and *Gfra2*$^{-/-}$ mice ($n = 3$, $p > 0.1$). However, the density of neuronal cells in myenteric plexus, as revealed by cuprolinic blue staining (data not shown), was slightly but significantly different between wild-type (410 ± 50) and *Gfra2*$^{-/-}$ duodena (310 ± 30 neurons per unit area, mean ± SEM, $n = 4$, $p < 0.05$). This suggests indirectly that AChE-positive neurons are reduced in number. Myenteric neurons can

be subdivided into different subpopulations according to their neurochemical composition and functional class. The myenteric layers are innervated by excitatory cholinergic, substance P-positive, and inhibitory noncholinergic vasoactive intestinal polypeptide– (VIP-) positive fibers, most of which are nitrergic in the small intestine (Sang and Young, 1998). AChE staining labels the majority of nonnitrergic myenteric neurons but is not specific for the cholinergic system. To address whether the lack of GFRα2 preferentially affects some specific subpopulation of enteric neurons, we stained thick sections of adult small bowel for these markers. Substance P-positive fibers were clearly reduced in *Gfra2*$^{-/-}$ mice, whereas the VIP-positive fibers appeared not to be affected by the mutation (n = 3; data not shown). Thus, the excitatory myenteric innervation is largely dependent on GFRα2-mediated signaling.

Analysis of α receptor expression in different parts of wild-type mouse gastrointestinal tract (Figure 4G) showed that *Gfra2* levels were highest at postnatal day 14, when *Gfra1* expression was barely detectable. Interestingly, *Gfra2* displayed variable expression levels along the gastrointestinal tract, being most prominent in the small bowel. The expression peak of *Gfra2* in wild-type mouse gut occurs at the time when development of cholinergic myenteric plexus is being accomplished (Vannucchi and Faussoni-Pelleggrini, 1996). Moreover, NTN levels are increased, while GDNF is very low in postnatal small intestine (Widenfalk et al., 1997; our unpublished data). At the same time, cholinergic innervation of the gut is reduced in both *Gfra2*$^{-/-}$ and *Ntn*$^{-/-}$ mice. Collectively, the data suggest that GFRα2-mediated signaling is essential for the development and maintenance of cholinergic innervation in the fine myenteric plexus.

Impaired Contractile Activity and Rhythm In Vitro

The less dense intestinal innervation of *Gfra2*$^{-/-}$ mutants prompted us to measure the contractile activity of their small intestine. The mutant mice displayed clear differences both in the duodenum (Figure 4H) and the ileum (Figure 4I) when compared to their wild-type littermates (n = 4 pairs). In the mutants, motility was constantly less pronounced and had a less organized pattern. There was a marked decrease in the mean amplitude of the tetrodotoxin- (TTX-) insensitive myogenic contractions and prolonged periods of relative quiescence; however, no difference in the frequency of the myogenic contractions was observed. The wild-type mice showed a periodic increase in motility combined with a prolonged contraction appearing every 6–8 min, which was markedly reduced, or absent, in *Gfra2*$^{-/-}$ animals. This pattern had a neuronal origin, as it was blocked by TTX (Figure 4I). A similar pattern has been described in the cat ileum, where the outflow of intestinal contents is correlated with this pattern (Weems and Seygal, 1981). Generation of these intrinsic propulsive patterns, normally observed to expel fluid, requires integrative mechanisms of the enteric nervous system, particularly the excitatory cholinergic motor neurons of the myenteric plexus (Goyal and Hirano, 1996). In line with a reduced innervation, the mutant ileum displayed a reduced response to electrical and pharmacological stimulation. Contractions induced by a supramaximal concentration of the cholinergic agonist carbachol (3 mM) in the mutant ileum were only 65%–84% (n = 3) of those observed in the wild-type siblings. Similarly, maximal contractions evoked by electrical stimuli in mutant ileum were 65%–71% (n = 3) of those in wild-type animals. Both the carbachol- and electrical stimulation–induced contractions were inhibited by TTX (data not shown). Methylene blue staining to reveal the interstitial cells of Cajal, which are the muscle-derived pacemaker cells of gut (Thomsen et al., 1998), failed to detect any differences between the genotypes (data not shown), supporting the conclusion that gut dysmotility of *Gfra2*$^{-/-}$ mice is mainly of neuronal origin. Future studies are needed to elucidate whether the mice have a deficient ascending contraction in vitro and impaired movement down the gut in vivo.

The expression peak of *Gfra2* in wild-type mouse gut (Figure 4A) correlated temporally with that of growth failure and spatially with the innervation defect in mutant animals. The reduced intestinal innervation and motility of *Gfra2*$^{-/-}$ mice imply gut dysfunction, which could contribute to their growth retardation. In addition, the onset of growth retardation at the beginning of solid food ingestion suggests that salivary gland dysfunction could also contribute to malnutrition and consequent poor growth. This hypothesis is supported by the finding that serum albumin was reduced by 15% in the mutants (*Gfra2*$^{-/-}$ 20 ± 3 mg/ml; wild-type 24 ± 3 mg/ml, n = 5 littermates, $p < 0.05$ using t test), whereas serum growth hormone was normal (*Gfra2*$^{-/-}$ 4.3 ± 2.0 ng/ml, n = 10; wild-type 4.0 ± 1.0 ng/ml, n = 11, ages 1.5–3 months). Reduced serum albumin levels and a relative preservation of brain size and body length are typically seen in humans who grow poorly due to malnutrition caused by abnormalities in the digestive tract (Mayer and Stern, 1992). Malnutrition can also result from poor feeding, and defects in alimentary tract function often secondarily lead to decreased food intake. However, we cannot exclude other mechanisms, central, endocrine, or metabolic, contributing to the growth failure. A strong expression of *Gfra2* in the hypothalamus (Figure 1D; Golden et al., 1998) is consistent with such a possibility. Therefore, analysis of feeding and more extensive screens on metabolic and endocrine parameters are warranted.

Reduced NTN- but Not GDNF-Induced Neuritogenesis of *Gfra2*$^{-/-}$ Trigeminal Explants

To analyze how the mutation affects GFRα2-signaling, we tested GDNF- and NTN-induced neurite outgrowth responses of E13 embryonic trigeminal ganglion explants, which express both *Gfra1* and *Gfra2* (Luukko et al., 1997). NTN (5 ng/ml) induced a prominent neuritic "halo" around the ganglion explants of wild-type mice (Figures 5A and 5I), whereas only a few neurites grew out from the explants of *Gfra2*$^{-/-}$ mice (Figures 5C and 5I). Interestingly, an intermediate level of neurite outgrowth was induced from ganglionic explants prepared from the *Gfra2*$^{+/-}$ mice (Figures 5B and 5I). With higher NTN concentrations (100 ng/ml), neurites became fasciculated or encircled the explants from wild-type ganglia (Figure 5E), which reduced the area of neurite outgrowth

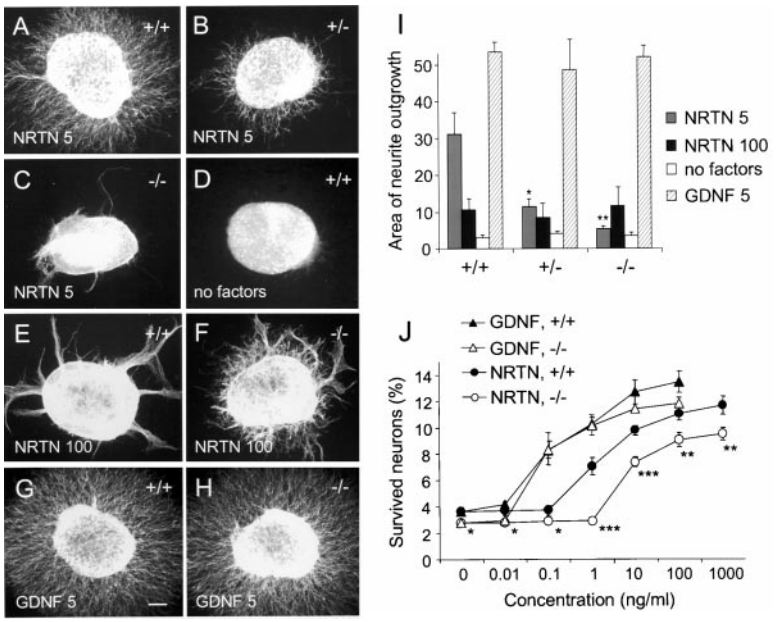

Figure 5. Neurite Outgrowth and Survival Responses of Trigeminal Ganglion Neurons from Wild-Type and *Gfra2*$^{-/-}$ Embryos to NTN or GDNF

(A–C) NTN (5 ng/ml) induces a robust fiber outgrowth from E13 trigeminal ganglion explants of wild-type mice (A). The neurite outgrowth response is clearly reduced in explants from *Gfra2*$^{+/-}$ mice (B) and almost absent in *Gfra2*$^{-/-}$ mice (C).

(D) No fiber outgrowth is seen from ganglia grown without added factors.

(E and F) Moderate neurite outgrowth is induced both from wild-type (E) and mutant (F) ganglia by higher NTN concentrations (100 ng/ml), the neurites being fasciculated or circled around the explants.

(G and H) Neurite outgrowth response to 5 ng/ml GDNF is robust both in wild-type (G) and *Gfra2*$^{-/-}$ (H) ganglia.

(I) Neurite outgrowth quantified from digitized images as the total area of neuronal processes. Numbers represent pixels per unit area ($\pm$ SD, n = 3–6 ganglia for each condition and genotype). **$p < 0.01$ between wild type and $-/-$, *$p < 0.05$ between the genotypes using t test.

(J) Survival (% of all plated $\pm$ SEM) of E14 trigeminal neurons in the presence of varying concentrations of GDNF or NTN. ***$p < 0.001$, **$p < 0.01$, *$p < 0.05$ between the genotypes using t test.

(Figure 5I). However, moderate neurite outgrowth was also induced from mutant ganglia with 100 ng/ml NTN (Figures 5F and 5I). GDNF (5 ng/ml) promoted an extensive neurite outgrowth from trigeminal ganglia explants of *Gfra2* mutant mice that appeared indistinguishable from that of the wild-type mice (Figures 5G–5I). Also, at a minimal concentration of GDNF (0.5 ng/ml), just enough to elicit a clear neurite response, no difference was observed between the genotypes (data not shown). As with NTN, a higher GDNF concentration (100 ng/ml) also evoked fiber fasciculation (data not shown).

Survival of *Gfra2*$^{-/-}$ Neurons in the Presence of NTN or GDNF

The requirement of GFRα2 for the trophic activities of NTN or GDNF was studied using dissociated trigeminal neurons (Figure 5J). While GDNF supported more neurons than NTN at lower concentrations, both factors at nearly saturating concentrations kept alive about 12% of plated neurons from wild-type mice. The survival response to GDNF corresponds with an earlier study (Henderson et al., 1994). In contrast with wild-type neurons, mutant neurons were about 10-fold less sensitive to NTN, whereas their response to GDNF was not statistically different. It is likely that both the neuritogenesis and survival promotion of mutant neurons at high NTN concentrations occurs via GFRα1, which has been shown to mediate NTN functions (Baloh et al., 1997; Buj-Bello et al., 1997; Creedon et al., 1997; Jing et al., 1997; Klein et al., 1997; Cacalano et al., 1998; Horger et al., 1998).

Although both *Ntn* and *Gdnf* are expressed in the target tissues of developing trigeminal neurons (Luukko et al., 1997, 1998), GDNF probably cannot replace the missing NTN/GFRα2 signaling in *Gfra2*$^{-/-}$ mice, since *Gfra1* and *Gfra2* may not be expressed by the same trigeminal neurons (Naveilhan et al., 1998). Direct counting of neuronal profiles from Nissl-stained paraffin sections of trigeminal ganglia did not reveal significant differences between adult wild-type and *Gfra2*$^{-/-}$ animals (-9%, n = 5, p = 0.4). A possible 10% (equivalent to the proportion of neurons expressing *Gfra2* in trigeminal ganglion) loss of neurons is probably too small to be detected by the counting method employed here. No significant losses of trigeminal neurons are found in *Gdnf*$^{-/-}$ (Moore et al., 1996) or *Gfra1*$^{-/-}$ (Cacalano et al., 1998) mice, although *Gfra1* expression in trigeminal ganglion neurons is reduced in *Gdnf*$^{-/-}$ mice (Naveilhan et al., 1998).

The number of superior cervical ganglion (SCG -11%, n = 4, p = 0.5) neurons was also not significantly different between adult wild-type and *Gfra2*$^{-/-}$ animals. Moreover, the nodose and dorsal root ganglia in *Gfra2*$^{-/-}$ mice appeared to be of equivalent size to those in wild-type animals (data not shown). Normal number of SCG neurons in *Gfra1*$^{-/-}$ (Cacalano et al., 1998; Enomoto et al., 1998), *Gfra2*$^{-/-}$ (this study), *Ntn*$^{-/-}$ (J. Milbrandt, personal communication), and only 30% loss in *Gdnf*$^{-/-}$ mice (Moore et al., 1996) contrasts with the complete lack of SCG in *Ret*$^{-/-}$ mice (Durbec et al., 1996a). Redundant coexpression of *Gfra1* and *Gfra2* in most SCG neurons and a complete promiscuity between GDNF and NTN in Ret activation via these coreceptors appears unlikely. This suggests a role for unknown factors and/or coreceptors that can activate Ret in sympathetic neuroblasts during SCG formation (Durbec et al., 1996a). For example, *Gfra3* is strongly expressed in embryonic and newborn mouse SCG neurons that are not supported by GDNF or NTN (our unpublished data).

Conclusions

We have shown that GFRα2 is absolutely required for development of several, but not all, postganglionic parasympathetic neurons. Our results agree with earlier in vitro data showing that GFRα2 is the primary receptor for NTN but not for GDNF and that NTN can also signal via GFRα1 at high concentrations (Baloh et al., 1997; Buj-Bello et al., 1997; Jing et al., 1997; Klein et al., 1997). The strikingly similar eye and gut phenotypes between *Gfra2*$^{-/-}$ and *Ntn*$^{-/-}$ mice (J. Milbrandt, personal communication) support the hypothesis that GFRα2 is the physiological NTN receptor in vivo and that NTN acts primarily as a target-derived factor for GFRα2-expressing neurons. The lack of obvious weight difference in NTN-deficient mice (J. Milbrandt, personal communication) suggests that the growth retardation in *Gfra2*$^{-/-}$ mice could be partially due to lack of NTN-independent signaling and that the enteric nervous system defect may not completely explain the growth failure of *Gfra2*$^{-/-}$ animals. However, it will be important to compare the phenotypes (for example, possible differences in salivary gland and gut innervation) and growths of the mice with the same genetic background and diet.

Requirement of GFRα2 and NTN for the postnatal development and maintenance of a subpopulation of enteric neurons contrasts the absolute requirement of Ret, GFRα1, and GDNF for the embryonic development of most enteric neurons (Schuchardt et al., 1994; Moore et al., 1996; Pichel et al., 1996; Sánchez et al., 1996; Cacalano et al., 1998; Enomoto et al., 1998). Based on the innervation defects and reduced albumin levels, we propose that growth retardation in *Gfra2*$^{-/-}$ mice results from salivary gland or enteric dysfunction leading to malnutrition. Hence, the mice may serve as a model for certain human parasympathetic nervous system disorders. In addition, mutations in *GFRα2* may contribute to human disorders involving the alimentary tract and lacrimal gland, such as dry eye syndromes and functional bowel diseases ranging from common recurrent abdominal pain to rare chronic intestinal pseudo-obstruction (Goyal and Hirano, 1996). Mutations in *RET* and *GDNF* have been found in children with Hirschsprung disease (aganglionic megacolon). Recently, heterozygous mutations in both *RET* and *NTN* were reported in severe cases of Hirschsprung disease with aganglionosis extending to the small intestine (Doray et al., 1998), supporting the crucial role of NTN-GFRα2 signaling in the development of the myenteric plexus of the small intestine.

Experimental Procedures

Generation of *Gfra2*$^{-/-}$ Mice

To isolate *Gfra2* genomic clones, we screened a mouse 129/Sv library (Stratagene) with a rat *Gfra2* cDNA probe (Suvanto et al., 1997). A 6.7 kb HindIII–XbaI fragment was used to construct the targeting vector (Figure 1A). A 0.5 kb NotI-XbaI fragment of the *Gfra2* gene, containing part of the first coding exon with the translation initiation site, was replaced with a 2.0 kb cassette containing the neomycin resistance gene (*neo*) driven by the *PGK* promoter and a polyadenylation signal (McBurney et al., 1991). R1 embryonic stem cells (Nagy et al., 1993) were electroporated with linearized vector and screened by Southern blot analysis (Figures 1A and 1B). Positive clones, identified at 1/40 frequency, were further hybridized with *neo* and 3′ outside probes to exclude random integration of the vector. Three injected clones gave germline transmission, when the chimeras were crossed to C57BL/6JOlaHsd or 129/SvHsd mice. Animals were genotyped by Southern blot or by PCR (Figure 1A) using primers P1, 5′-CACATACACACAAAACTGTGGG-3′; P2, 5′-ATTCGCAGCGCATCGCCTTC-3′; and common P3, 5′-ATGTTGGAAGTCTCCTTCTCG-3′. Primer pairs P1/P3 and P2/P3 give specific PCR products for the wild-type and mutant alleles, respectively. If not otherwise stated, littermates of the same sex from heterozygote matings in the hybrid 129/Sv × C57BL/6 background were used. To quantitate growth, the body weight and nose–tail length of *Gfra2*$^{-/-}$ and wild-type mice from several litters were recorded weekly from birth up to 6 months.

Northern Blot and RT–PCR Analysis of *Gfra* mRNAs

Total RNA extraction and Northern blot was carried out as described previously (Reeben et al., 1998). The blot was hybridized with probes specific for mouse *Gfra2* (a PCR fragment of nucleotides 1–570; Baloh et al., 1997), *Gfra1* (a 777 bp EST AF012811), and *Ret* (3.3 kbp of X67812; Pachnis et al., 1993).

The cDNA clones representing the 5′ region of the short *Gfra2* transcript were obtained by 5′-RACE procedure. Briefly, the total RNA from *Gfra2*$^{-/-}$ brains was reverse transcribed, oligo(dA) tailed, and amplified with primer oligo(dT) and a reverse primer corresponding to exon 2, 5′-GCTTTCCTGCAAGACCTCCAG-3′. After a second round of amplification with oligo(dT) and nested primer 5′-AGCCGCACACAGCTCATTGG−3′, the products were cloned and sequenced in both orientations.

For RT–PCR analysis of *Gfra1* and *Gfra2* expression in gastrointestinal tract, total RNA was reverse transcribed and amplified for 36 cycles (95°C for 45 s, 62°C for 45 s, and 72°C for 60 s). The amounts of total RNA in samples were normalized by amplification of a *Ppia* (alias *cyclophilin*) fragment using commercial primers (Ambion). Amplification with 40 cycles gave qualitatively similar results, indicating that the result from 36 cycles was in the linear range. The primers were *Gfra1*, 5′-GCGGCACCATGTTCCTAGCC−3′ and 5′-CAGACTCAGGCAGTTGGGCC-3′; and *Gfra2*, 5′-TATTGGAGCATCCATCTGGG-3′ and 5′-AGCAGTTGGGCTTCTCCTTG-3′. Product sizes were 746 and 429 bp for *Gfra1* and *Gfra2*, respectively.

In Situ Hybridization

Fresh frozen tissues were sectioned at 14 μm and fixed in 4% paraformaldehyde (PFA) for 15 min. In situ hybridization using ^{35}S-labeled RNA probes for *Ret*, *Gdnf*, *Ntn*, *Gfra1*, and *Gfra2* (Luukko et al., 1997, 1998; Suvanto et al., 1997) was performed as described (Reeben et al., 1998). Template for *Gfra2* exon 1 probe was a 424 bp EST (AA048808 WashU-HHMI Mouse EST Project).

Histology

Anesthetized animals were perfused intracardially with PBS followed by 4% PFA for a few minutes. A length of the oculomotor nerve was dissected, postfixed in 2% glutaraldehyde, and embedded in epon. Semithin sections were stained with toluidine blue, and the myelinated axon profiles were drawn to produce mean axon diameters. Gut samples (removed directly or after perfusion with PBS) were opened along their mesenteric border, washed in PBS, pinned on silicone without stretching, and postfixed in PFA for 2 hr. The mucosal layer was removed, and the muscle layer was whole-mount stained for AChE as described (Tago et al., 1986), except that 1% Triton X−100 was included in the staining solution to increase penetration. Adjacent parts were stained for NADPH-diaphorase histochemistry as described (Vincent, 1992). The density of positive fibers in the myenteric plexus was quantified with 20× magnification by counting fibers crossing a standardized grid from four positions per sample. To estimate the total number of neurons in myenteric ganglia, the muscle layer was whole-mount stained with Cuprolinic blue (Heinicke et al., 1987). All cells with a clear nucleus were counted from three positions along a band (of 20× field width) throughout the entire circumference of the duodenum.

For immunohistochemistry, lengths of small intestine were flat frozen and 50 μm sections cut tangentially through the muscle layer. Sections were stained and detected by using standard immunofluorescence techniques. Primary antibodies were against PGP9.5 (rabbit polyclonal, UltraClone), substance P (rat monoclonal NC1, Medicorp), TH (rabbit polyclonal P40101-0, Pel-Freez), ChAT (goat polyclonal AB144P, Chemicon), VAChT (goat polyclonal AB1578,

Chemicon), and VIP (rabbit polyclonal VA 1285, Affiniti). Paraffin sections were stained with hematoxylin and eosin or cresyl violet and neuronal profiles with a clear nucleolus counted from every fifth or tenth section.

Lacrimal Gland Secretion

Mice (3- to 5-month-old littermates) were mildly anesthetized with Avertin. Tear secretion was estimated by a modified Schirmer test (Humphreys-Beher et al., 1994). Briefly, a pH indicator paper strip (width 1.5 mm) was placed on the medial angle of the eye for 1 min, and the length of the wet portion was measured.

Contractile Activity of Gut In Vitro

Mice were killed, and the lengths of ileum and duodenum (3 cm) were dissected, cleaned, and suspended in a Tyrode's solution at 32°C (containing [in mM]: NaCl 124, KCl 2.7, $MgCl_2$ 0.5, $CaCl_2$ 1.4, NaH_2PO_4 0.4, $NaHCO_3$ 25, glucose 5.6; continuously gassed with 5% CO_2/95% O_2). The contractile activity was measured with a Grass FT03 force displacement transducer coupled to a polygraph and digitized for off line analysis. Following recordings of spontaneous contractile activity, electrical stimulation (50 V, 0.2 ms duration at 0.5–64 Hz for 10 s) was done using Grass S 48 stimulators and parallel platinum electrodes (16 mm long, 6 mm apart). A maximal contraction was achieved with 32 Hz in both wild-type and *Gfra2*$^{-/-}$ animals. The contractions induced by carbachol and electrical stimulation were completely inhibited by 0.5 μM TTX.

Serum Albumin and Growth Hormone Measurements

Blood samples were taken intracardially from anesthetized animals. Serum albumin was measured in the laboratory of Helsinki University Hospital. Serum growth hormone (GH) concentrations were determined by a radioimmunoassay using a rat GH kit (a gift from the National Institute of Diabetes and Digestive and Kidney Diseases) according to the instructions and expressed in nanograms per milliliter of NIDDK-GH-RP−2 standard.

Ganglion Explant Culture

E13–E14 mouse trigeminal ganglia were prepared and cultured in collagen matrix as described (Ebendal, 1989; Arumäe et al., 1993). Recombinant GDNF, NTN, or NGF (PeproTech), or GDNF kindly donated by Cephalon were applied at concentrations ranging from 0.5 to 100 ng/ml. The explants were cultured for 48 hr, fixed, and stained with neurofilament antibodies as described (Arumäe et al., 1993). The media had no neurite outgrowth–promoting activity (Figure 5D). The magnitude of neurite outgrowth was scored from digitized images using ImageProPlus software. After excluding the area of ganglion body, the area covered by neurites was measured automatically as the number of pixels above background level.

Neuronal Survival Assay

E14 (±1) trigeminal ganglia from separate wild-type and *Gfra2*$^{-/-}$ litters were digested by trypsin, and the nonneuronal cells were removed by preplating, yielding almost pure neuronal cultures. The neurons were plated onto 4-well tissue culture dishes coated with poly-L-ornithine and laminin. F−14 medium containing serum substitute and standard antibiotics was used for preplating and culturing (Davies, 1995). The cultures received GDNF, NTN, or NGF at different concentrations. After 30–35 hr, when 95%–98% of the control neurons grown without added growth factors were dead, the neurons were fixed. All phase-bright healthy neurons with intact neurites were counted. Wild-type and *Gfra2*$^{-/-}$ neurons responded dose dependently and similarly to NGF. More than 90% of neurons were maintained by 2 ng/ml NGF (data not shown). The results were expressed as a percent from initially plated neurons (neurons maintained 10–12 hr in the presence of the cocktail of NGF, GDNF, and NTN). The results are from three independent experiments, with all experimental points carried out in duplicate.

Acknowledgments

We thank E. Kujamäki for performing the in situ hybridizations; S. Åkerberg for the histology; L. Viinikka for the blood tests; A. Nagy for the ES cells; M. Moshnyakov, P. Suvanto, C. Ibáñez, and V. Pachnis for probes; the staff of the Viikki Laboratory Animal Center for animal care; D. Rice for linguistic revision; and H. Sariola, E. Klinge, and T. Kivelä for helpful discussions. We are indebted to J. Milbrandt for communicating results prior to publication and useful comments to the manuscript. This work was supported by the Academy of Finland, Biocentrum Helsinki, Cephalon, EU Biomed (grant BMH4–97–2157), and the Sigrid Juselius Foundation. M. S. is a fellow of Biocentrum Helsinki.

Received September 11, 1998; revised December 11, 1998.

References

Arumäe, U., Pirvola, U., Palgi, J., Kiema, T.R., Palm, K., Moshnyakov, M., Ylikoski, J., and Saarma, M. (1993). Neurotrophins and their receptors in rat peripheral trigeminal system during maxillary nerve growth. J. Cell Biol. *122*, 1053–1065.

Baloh, R.H., Tansey, M.G., Golden, J.P., Creedon, D.J., Heuckeroth, R.O., Keck, C.L., Zimonjic, D.B., Popescu, N.C., Johnson, E.M., Jr., and Milbrandt, J. (1997). TrnR2, a novel receptor that mediates neurturin and GDNF signaling through Ret. Neuron *18*, 793–802.

Baloh, R.H., Gorodinsky, A., Golden, J.P., Tansey, M.G., Keck, C.L., Popescu, N.C., Johnson, E.M., Jr., and Milbrandt, J. (1998a). GFRα3 is an orphan member of the GDNF/neurturin/persephin receptor family. Proc. Natl. Acad. Sci. USA *95*, 5801–5806.

Baloh, R.H., Tansey, M.G., Lampe, P.A., Fahner, T.J., Enomoto, H., Simburger, K.S., Leitner, M.L., Araki, T., Johnson, E.M., Jr., and Milbrandt, J. (1998b). Artemin, a novel member of the GDNF ligand family, supports peripheral and central neurons and signals through the GFRα3-RET receptor complex. Neuron *21*, 1291–1302.

Buj-Bello, A., Buchman, V.L., Horton, A., Rosenthal, A., and Davies, A.M. (1995). GDNF is an age-specific survival factor for sensory and autonomic neurons. Neuron *15*, 821–828.

Buj-Bello, A., Adu, J., Piñon, L.G., Horton, A., Thompson, J., Rosenthal, A., Chinchetru, M., Buchman, V.L., and Davies, A.M. (1997). Neurturin responsiveness requires a GPI-linked receptor and the Ret receptor tyrosine kinase. Nature *387*, 721–724.

Cacalano, G., Farinas, I., Wang, L., Hagler, K., Forgie, A., Moore, M., Armanini, M., Phillips, H., Ryan, A.M., Reichardt, L., et al. (1998). GFRα1 is an essential receptor component for GDNF in the developing nervous system and kidney. Neuron *21*, 53–62.

Creedon, D.J., Tansey, M.G., Baloh, R.H., Osborne, P.A., Lampe, P.A., Fahrner, T.J., Heuckeroth, R.O., Milbrandt, J., and Johnson, E.M., Jr. (1997). Neurturin shares receptors and signal transduction pathways with glial cell line–derived neurotrophic factor in sympathetic neurons. Proc. Natl. Acad. Sci. USA *94*, 7018–7023.

Davies, A.M. (1995). Cranial sensory neurons. In Neural Cell Culture, J. Cohen and G.P. Wilkin, eds. (Oxford: Oxford University Press), pp. 153–175.

Doray, B., Salomon, R., Amiel, J., Pelet, A., Touraine, R., Billaud, M., Attié, T., Bachy, B., Munnich, A., and Lyonnet, S. (1998). Mutation of the RET ligand, neurturin, supports multigenic inheritance in Hirschsprung disease. Hum. Mol. Genet. *7*, 1449–1452.

Durbec, P.L., Larsson-Blomberg, L.B., Schuchardt, A., Costantini, F., and Pachnis, V. (1996a). Common origin and developmental dependence on c-ret of subsets of enteric and sympathetic neuroblasts. Development *122*, 349–358.

Durbec, P., Marcos-Gutierrez, C.V., Kilkenny, C., Grigoriou, M., Wartiowaara, K., Suvanto, P., Smith, D., Ponder, B., Costantini, F., Saarma, M., et al. (1996b). GDNF signaling through the Ret receptor tyrosine kinase. Nature *381*, 789–793.

Ebendal, T. (1989). Use of collagen gels to bioassay nerve growth factor activity. In Nerve Growth Factors, R.A. Rush, ed. (Chichester, UK: John Wiley and Sons, Ltd.), pp. 81–93.

Enokido, Y., de Sauvage, F., Hongo, J.-A., Ninika, N., Rosenthal, A., Buchman, V.L., and Davies, A.M. (1998). GFRα4 and the tyrosine kinase Ret form a functional receptor complex for persephin. Curr. Biol. *8*, 1019–1022.

Enomoto, H., Araki, T., Jackman, A., Heuckeroth, R., Snider., W.D., Johnson, E.M., and Milbrandt, J. (1998). GFRα1-deficient mice have

deficits in the enteric nervous system and kidneys. Neuron *21*, 317–324.

Golden, J.P., Baloh, R.H., Kotzbauer, P.T., Lampe, P.A., Osborne, P.A., Milbrandt, J., and Johnson, E.M., Jr. (1998). Expression of neurturin, GDNF, and their receptors in the adult mouse CNS. J. Comp. Neurol. *398*, 139–150.

Goyal, R.K., and Hirano, I. (1996). Mechanisms of disease: the enteric nervous system. N. Engl. J. Med. *334*, 1106–1115.

Heinicke, E.A., Kiernan, J.A., and Wijsman, J. (1987). Specific, selective and complete staining of neurons of the myenteric plexus, using Cuprolinic blue. J. Neurosci. Methods *21*, 45–54.

Henderson, C.E., Phillips, H.S., Pollock, R.A., Davies, A.M., Lemeulle, C., Armanini, M., Simmons, L., Moffet, B., Vandlen, R.A., Simmons, L., et al. (1994). GDNF: a potent survival factor for motoneurons present in peripheral nerve and muscle. Science *266*, 1062–1064.

Horger, B.A., Nishimura, M.C., Armanini, M.P., Wang, L.C., Poulsen, K.T., Rosenblad, C., Kirik, D., Moffat, B., Simmons, L., Johnson, E., Jr., et al. (1998). Neurturin exerts potent actions on survival and function of midbrain dopaminergic neurons. J. Neurosci. *18*, 4929–4937.

Humphreys-Beher, M.G., Hu, Y., Nakagawa, Y., Wang, P.-L., and Purushotham, K.R. (1994). Utilization of the nonobese diabetic (NOD) mouse as an animal model for the study of secondary Sjögren's syndrome. Adv. Exp. Med. Biol. *350*, 631–636.

Jing, S., Wen, D., Yu, Y., Holst, P.L., Luo, Y., Fang, M., Tamir, R., Antonio, L., Hu, Z., Cupples, R., et al. (1996). GDNF-induced activation of the ret protein tyrosine kinase is mediated by GDNFR-α, a novel receptor for GDNF. Cell *85*, 1113–1124.

Jing, S., Yu, Y., Fang, M., Hu, Z., Holst, P.L., Boone, T., Delaney, J., Schultz, H., Zhou, R., and Fox, G.M. (1997). GFRα-2 and GFRα-3 are two new receptors for ligands of the GDNF family. J. Biol. Chem. *272*, 33111–33117.

Klein, R.D., Sherman, D., Ho, W.H., Stone, D., Bennett, G.L., Moffat, B., Vandlen, R., Simmons, L., Gu, Q., Hongo, J.A., et al. (1997). A GPI-linked protein that interacts with Ret to form a candidate neurturin receptor. Nature *387*, 717–721.

Kotzbauer, P.T., Lampe, P.A., Heuckeroth, R.O., Golden, J.P., Creedon, D.J., Johnson, E.M., Jr., and Milbrandt, J. (1996). Neurturin, a relative of glial-cell-line-derived neurotrophic factor. Nature *384*, 467–470.

Lin, L.F., Doherty, D.H., Lile, J.D., Bektesh, S., and Collins, F. (1993). GDNF: a glial cell line–derived neurotrophic factor for midbrain dopaminergic neurons. Science *260*, 1130–1132.

Luukko, K., Suvanto, P., Saarma, M., and Thesleff, I. (1997). Expression of GDNF and its receptors in developing tooth is developmentally regulated and suggests multiple roles in innervation and organogenesis. Dev. Dyn. *210*, 463–471.

Luukko, K., Saarma, M., and Thesleff, I. (1998). Neurturin mRNA expression suggests roles in trigeminal innervation of the first branchial arch and in tooth formation. Dev. Dyn. *213*, 207–219.

Masure, S., Cik, M., Pangalos, M.N., Bonaventure, P., Verhasselt, P., Lesage, A.S., Leysen, J.E., and Gordon, R.D. (1998). Molecular cloning, expression and tissue distribution of glial-cell-line-derived neurotrophic factor family receptor α-3 (GFRα-3). Eur. J. Biochem. *251*, 622–630.

Mayer, E., and Stern, E. (1992). Growth failure in gastrointestinal diseases. Bailliere's Clin. Endocrinol. Metab. *6*, 645–659.

McBurney, M.W., Sutherland, L.C., Adra, C.N., Leclair, B., Rudnicki, M.A., and Jardine, K. (1991). The mouse Pgk−1 gene promoter contains an upstream activator sequence. Nucleic Acids Res. *19*, 5755–5761.

Milbrandt, J., de Sauvage, F.J., Fahrner, T.J., Baloh, R.H., Leitner, M.L., Tansey, M.G., Lampe, P.A., Heuckeroth, R.O., Kotzbauer, P.T., Simburger, K.S., et al. (1998). Persephin, a novel neurotrophic factor related to GDNF and neurturin. Neuron *20*, 245–253.

Moore, M.W., Klein, R.D., Farinas, I., Sauer, H., Armanini, M., Phillips, H., Reichardt, L.F., Ryan, A.M., Carver-Moore, K., and Rosenthal, A. (1996). Renal and neuronal abnormalities in mice lacking GDNF. Nature *382*, 76–79.

Nagy, A., Rossant, J., Nagy, R., Abramow-Newerly, W., and Roder, J.C. (1993). Derivation of completely cell culture–derived mice from early-passage embryonic stem cells. Proc. Natl. Acad. Sci. USA *90*, 8424–8428.

Naveilhan, P., Baudet, C., Mikaels, A., Shen, L., Westphal, H., and Ernfors, P. (1998). Expression and regulation of GFRα3, a glial cell line–derived neurotrophic factor family receptor. Proc. Natl. Acad. Sci. USA *95*, 1295–1300.

Nomoto, S., Ito, S., Yang, L.X., and Kiuchi, K. (1998). Molecular cloning and expression analysis of GFRα-3, a novel cDNA related to GDNFRα and NRTNRα. Biochem. Biophys. Res. Commun. *244*, 849–853.

Nosrat, C.A., Tomac, A., Hoffer, B.J., and Olson, L. (1997). Cellular and developmental patterns of expression of Ret and glial cell line–derived neurotrophic factor receptor alpha mRNAs. Exp. Brain Res. *115*, 410–422.

Pachnis, V., Mankoo, B., and Costantini, F. (1993). Expression of the c-ret proto-oncogene during mouse embryogenesis. Development *119*, 1005–1017.

Pichel, J.G., Shen, L., Sheng, H.Z., Granholm, A.C., Drago, J., Grinberg, A., Lee, E.J., Huang, S.P., Saarma, M., Hoffer, B.J., et al. (1996). Defects in enteric innervation and kidney development in mice lacking GDNF. Nature *382*, 73–76.

Reeben, M., Laurikainen, A., Hiltunen, J.O., Castrén, E., and Saarma, M. (1998). The messenger RNAs for both glial cell line–derived neurotrophic factor receptors, *c-Ret* and GDNFRα, are induced in the rat brain. Neuroscience *83*, 151–159.

Sánchez, M.P., Silos-Santiago, I., Frisen, J., He, B., Lira, S.A., and Barbacid, M. (1996). Renal agenesis and the absence of enteric neurons in mice lacking GDNF. Nature *382*, 70–73.

Sang, Q., and Young, H.M. (1998). The identification and chemical coding of cholinergic neurons in the small and large intestine of the mouse. Anat. Rec. *251*, 185–199.

Sanicola, M., Hession, C., Worley, D., Carmillo, P., Ehrenfels, C., Walus, L., Robinson, S., Jaworski, G., Wei, H., Tizard, R., et al. (1997). Glial cell line–derived neurotrophic factor–dependent RET activation can be mediated by two different cell-surface accessory proteins. Proc. Natl. Acad. Sci. USA *94*, 6238–6243.

Schuchardt, A., D'Agati, V., Larsson-Blomberg, L., Costantini, F., and Pachnis, V. (1994). Defects in the kidney and enteric nervous system of mice lacking the tyrosine kinase receptor Ret. Nature *367*, 380–383.

Suvanto, P., Hiltunen, J.O., Arumäe, U., Moshnyakov, M., Sariola, H., Sainio, K., and Saarma, M. (1996). Localization of glial cell line–derived neurotrophic factor (GDNF) mRNA in embryonic rat by in situ hybridization. Eur. J. Neurosci. *8*, 816–822.

Suvanto, P., Wartiovaara, K., Lindahl, M., Arumäe, U., Moshnyakov, M., Horelli-Kuitunen, N., Airaksinen, M.S., Palotie, A., Sariola, H., and Saarma, M. (1997). Cloning, mRNA distribution and chromosomal localization of the gene for glial cell line–derived neurotrophic factor receptor-β, a homologue to GDNFR-α. Hum. Mol. Genet. *6*, 1267–1273.

Tago, H., Kimura, H., and Maeda, T. (1986). Visualization of detailed acetylcholinesterase fiber and neuron staining in rat brain by a sensitive histochemical procedure. J. Histochem. Cytochem. *34*, 1431–1438.

Thompson, J., Doxakis, E., Pïnon, L.G.P., Strachan, P., Buj-Bello, A., Wyatt, S., Buchman, V.L., and Davies, A.M. (1998). GFRα-4, a new GDNF family receptor. Mol. Cell. Neurosci. *11*, 117–126.

Thomsen, L., Robinson, T.L., Lee, J.C., Farraway, L.A., Hughes, M.J., Andrews, D.W., and Huizinga, J.D. (1998). Interstitial cells of Cajal generate a rhythmic pacemaker current. Nature Med. *4*, 848–851.

Treanor, J.J., Goodman, L., de Sauvage, F., Stone, D.M., Poulsen, K.T., Beck, C.D., Gray, C., Armanini, M.P., Pollock, R.A., Hefti, F., et al. (1996). Characterization of a multicomponent receptor for GDNF. Nature *382*, 80–83.

Trupp, M., Ryden, M., Jornvall, H., Funakoshi, H., Timmusk, T., Arenas, E., and Ibáñez, C.F. (1995). Peripheral expression and biological activities of GDNF, a new neurotrophic factor for avian and mammalian peripheral neurons. J. Cell Biol. *130*, 137–148.

Trupp, M., Arenas, E., Fainzilber, M., Nilsson, A.S., Sieber, B.A.,

Grigoriou, M., Kilkenny, C., Salazar-Grueso, E., Pachnis, V., Arumäe, U., et al. (1996). Functional receptor for GDNF encoded by the c-ret proto-oncogene. Nature *381*, 785–788.

Trupp, M., Belluardo, N., Funakoshi, H., and Ibáñez, C.F. (1997). Complementary and overlapping expression of glial cell line–derived neurotrophic factor (GDNF), c-ret proto-oncogene, and GDNF receptor-alpha indicates multiple mechanisms of trophic actions in the adult rat CNS. J. Neurosci. *17*, 3554–3567.

Trupp, M., Raynoschek, C., Belluardo, N., and Ibáñez, C.F. (1998). Multiple GPI-anchored receptors control GDNF-dependent and independent activation of the c-ret receptor tyrosine kinase. Mol. Cell. Neurosci. *11*, 47–63.

Vannucchi, M.G., and Faussoni-Pellegrini, M.S. (1996). Differentiation of cholinergic cells in the rat gut during pre- and postnatal life. Neurosci. Lett. *206*, 105–108.

Vincent, S.R. (1992). Histochemistry of endogenous enzymes. In Experimental Neuroanatomy, a Practical Approach, J.P. Bolam, ed. (Oxford: IRL Press), pp. 162–164.

Weems, W.A., and Seygal, G.E. (1981). Fluid propulsion by cat intestinal segments under conditions requiring hydrostatic work. Am. J. Physiol. *240*, G147–G156.

Widenfalk, J., Nosrat, C., Tomac, A., Westphal, H., Hoffer, B., and Olson, L. (1997). Neurturin and glial cell line–derived neurotrophic factor receptor-β (GDNFR-β), novel proteins related to GDNF and GDNFR-α with specific cellular patterns of expression suggesting roles in the developing and adult nervous system and in peripheral organs. J. Neurosci. *17*, 8506–8519.

Worby, C.A., Vega, Q.C., Chao, H.H., Seasholtz, A.F., Thompson, R.C., and Dixon, J.E. (1998). Identification and characterization of GFRα-3, a novel coreceptor belonging to the glial cell line–derived neurotrophic receptor family. J. Biol. Chem. *273*, 3502–3508.

Yu, T., Scully, S., Yu, Y., Fox, G.M., Jing, S., and Zhou, R. (1998). Expression of GDNF family receptor components during development: implications in the mechanisms of interaction. J. Neurosci. *18*, 4684–4696.